Project Closing, Final Report

NKFIH OTKA K128985, PI: Győző Garab

"Lipid polymorphism of thylakoid membranes. Structural entities, membrane dynamics, photosynthetic functions"

Major aims and questions of the research

In this project we addressed one of the basic, enigmatic questions of membrane biology and bioenergetics: the role of non-bilayer lipids and non-lamellar lipid phases in the structure and function of plant thylakoid membranes (TMs).

The most important goal of our research was to extend the 'standard' fluid-mosaic bilayer membrane model of Singer and Nicolson (1972) – to allow the presence of non-bilayer lipid species in biological membranes and to explain the structural and functional roles of the earlier observed non-lamellar lipid phases in fully functional isolated plant TMs (Krumova et al. 2008 a,b; Garab et al. 2017). Plant TMs are globally important light-energy converting membranes.

During the course of the project, we have found the opportunity for collaborative works on the role of non-bilayer lipids and non-lamellar lipid phases in the inner mitochondrial membranes (IMMs), the other main energy-converting membranes of the Biosphere, which have been shown to exhibit marked lipid polymorphism associated with the synthesis of ATP (Gasanov et al. 2018). Thus, in the Report, while focusing on the lipid polymorphism of TMs, the relevant basic questions on IMMs, will also be considered.

The Final Report will focus on the above identified fundamental questions of lipid polymorphism in TMs and IMMs, and on DEM, the dynamic exchange model of energy-converting membranes (Section 1). Results on lipid-protein interactions, primarily but not exclusively, in photosynthetic pigment-protein complexes and in supercomplexes, and on the (macro-)organization of TMs will be assessed as well as publications of methodological relevance will only briefly reviewed (Section 2). In general, the Final Report intends to provide an overview of the works, rather than to repeat the summaries of the published papers – which had been given in the annual reports.

1. Structural and functional roles of non-lamellar lipid phases in TMs and IMMs

In the following, introductory chapters, I follow the scheme of presentation, in condensed form and omitting most references, as published in (Garab et al. 2022 – listed). The purpose of these paragraphs is to provide a background information on TMs and IMMs – focusing on common structural and functional motifs that are related to the high abundance of non-bilayer lipids in these membrane systems and to the observed strong lipid polymorphisms.

1.1. Introduction. TMs and IMMs: similarities and differences

Photosynthesis and respiration are, in essence, opposite processes. Nevertheless, chloroplasts and mitochondria possess a number of important features in common. Concerning their cellular role, both chloroplasts and mitochondria are semi-autonomous organelles. Regarding their basic ultrastructure, they are surrounded by outer membranes, the chloroplast envelope membranes, and the outer mitochondrial membrane (OMM), respectively; and contain inner membranes, the TMs and the IMMs. The double envelope membranes of plant chloroplasts have been shown to form a dynamic interface between plastids and the cytosol. Very similar functions – regulation of mitochondrial homeostasis by coordinating mitochondrial dynamics and quality control – are performed by specific OMM proteins. Neither the chloroplast envelope membranes nor OMM participate directly in the processes of energy conversion. The energy-transducing functions of chloroplasts and mitochondria are performed by their inner membranes, i.e. by TMs and IMMs.

1.1.1. Components of the electron transport chains

In oxygenic photosynthetic organisms, the light reactions of photosynthesis occur in TMs, flattened membrane vesicles, which, in chloroplasts, separate the inner, lumenal, and the outer, stromal side, aqueous phases (Fig. 1a). They embed the two photosystems (PSs): PSII (the water-plastoquinone oxidoreductase) and PSI (the plastocyanin–ferredoxin oxidoreductase), along with their associated light-harvesting antenna complexes (in green plants, LHCII and LHCI, respectively). They also accommodate the cytochrome b6f complex (cyt bf, plastoquinol-plastocyanin oxidoreductase). Further constituents of the photosynthetic electron transport chain (ETC) are the mobile electron carrier molecules, the pool of plastoquinone molecules, transferring reducing equivalents inside the lipid phase of TMs from PSII toward the cyt bf, and the lumenal mobile electron carrier protein plastocyanin, acting between the cyt bf complex and PSI. Also associated with the membrane, but not accommodated in it, are the water-splitting enzyme or oxygen evolving complex (OEC), at the lumenal-side of PSII, and the ferredoxin (Fd) and the ferredoxin:NADP oxidoreductase (FNR), at the stromal side of PSI. The TMs also contain the ATP synthase, with its Fo and F1 units, respectively, embedded in the lipid membrane and protruding deeply into the outer, stroma-side aqueous phase.

IMMs also contain virtually all components of the ETC – the respiratory chain. IMM separates the inner aqueous phase, the mitochondrial matrix, from the outer aqueous phase, the intermembrane space between OMM and IMM (Fig. 1b). IMMs contain the respiratory protein complexes I-IV: CI (Complex I, the NADH:ubiquinone (NADH:UQ) oxidoreductase), CII (Complex II, succinate dehydrogenase or succinate-coenzyme Q reductase), CIII (Complex III, ubiquinol-cytochrome *c* reductase or cytochrome *bc1* complex, cyt *bc*) and CIV (Complex IV, cytochrome *c* oxidase). As in TMs, the two major complexes of the mitochondrial respiratory ETC, CI and CII, possess large protein subunits protruding into the aqueous phase, into the matrix. They also contain two mobile compounds: the lipophylic ubiquinone (UQ) molecules transfer reducing equivalents between CI/CII and CIII; and the water-soluble electron carrier protein, cytochrome *c* (cyt *c*), transfers electrons along the membrane surface in the outer, intermembrane aqueous phase, from CIII to CIV. IMM also contains Complex V, the FoF1-ATP synthase, with its large F1 unit protruding into the matrix, i.e. the inner aqueous phase.

1.1.2. Electron transport and the associated proton transport

In TMs, the events of the primary charge separations in the two photochemical reaction centers (RCs), supplied with excitation energy by antenna complexes, are followed by vectorial electron transport processes from water to $NADP^+$ (Fig. 1a). The operation of the ETC is linked to proton transport. Protons arising from water splitting are deposited into the lumen during the operation of the OEC; and are taken up from the outer aqueous phase during the reduction of the PSII secondary quinone acceptor QB, i.e. upon the formation of QBH_2. After the release of QBH_2 (a plastoquinol molecule, PQH_2) and its diffusion from PSII to the plastoquinol-binding site of the cyt bf complex, protons are released at the lumenal side, while the reduction of $NADP^+$ is coupled with proton uptake from the outer aqueous phase. These processes lead to the evolution of molecular oxygen, and the synthesis of NADPH, and generate an electrochemical potential gradient for protons ($\Delta\mu_{H^+}$), or proton-motive force (pmf) (Fig. 1a).

During the electron-transport processes in IMM, electrons are shuffled from CI and CII via CIII to CIV; these processes are assisted by the mobile ETC components (UQ and cyt c). In general, the ETC reactions are coupled to proton transport: protons are pumped by CI from the matrix into the intermembrane space and are released there upon the CIII-catalyzed oxidation of UQH_2. These processes lead to the oxidation of NADH and succinate, the consumption of O_2 and the release of H_2O; and generate pmf (Fig. 1b).

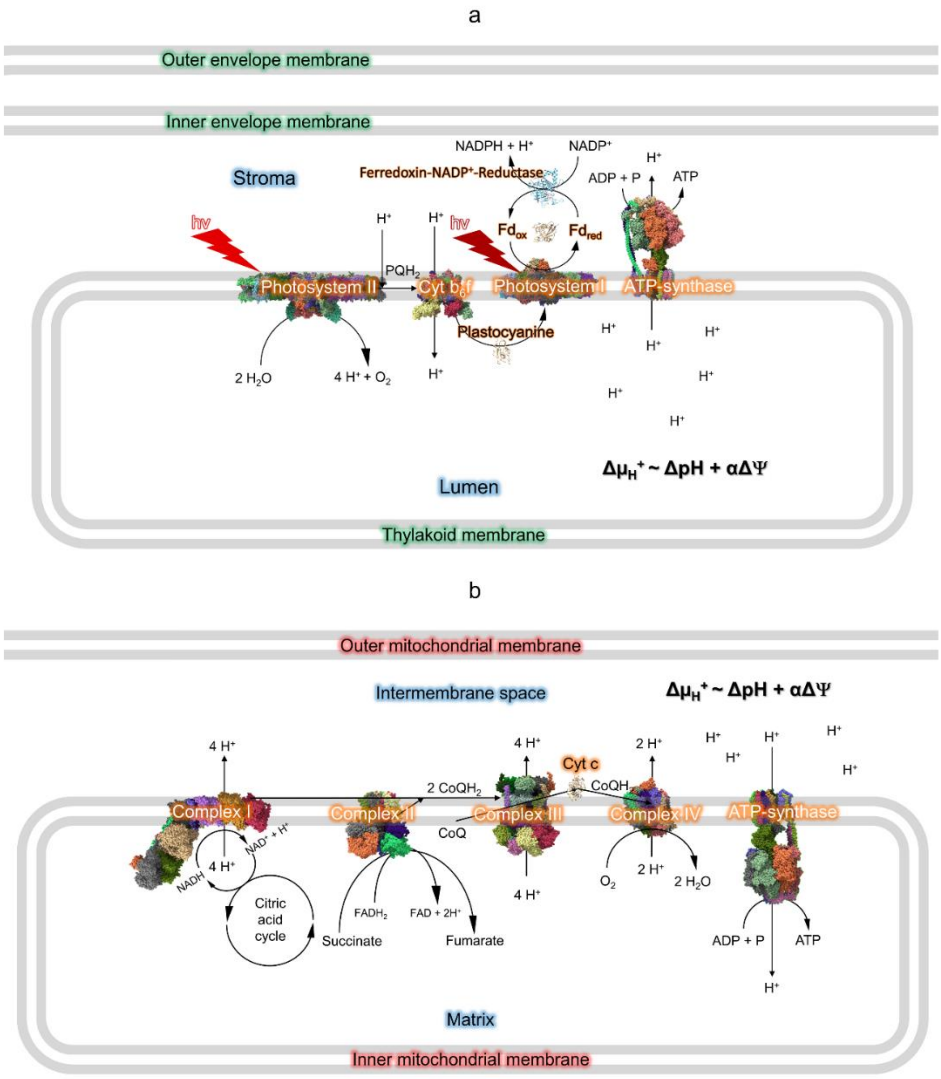

Fig. 1. Schematic representation of the photosynthetic (a) and mitochondrial (b) ETCs and ATP synthases. The electron and proton transfer processes are symbolized by arrows, in most cases with no attention to the stoichiometries.

1.1.3. Membrane energization and ATP synthesis

In TM, $\Delta\mu_H^+$, generated by the primary charge separation and the consecutive vectorial electron and proton transport processes, consists of a transmembrane ΔpH (of 2-3 pH units) and an electric potential gradient (ΔΨ) across the membrane (corresponding to a field strength of ~10^5 V cm^{-1}); the positive side is the lumenal, inner aqueous side.

The $\Delta\mu_H^+$ across IMM, generated by the vectorial electron transport coupled with proton pumps/depositions into the intermembrane space (Fig. 1b) also has two components, the electrical component that is caused by a charge difference across the lipid membrane, and a chemical component due to a differential concentration of ions and H^+ ions, in particular. The magnitude of this electrochemical membrane potential difference is about 200 mV, similar to that in TMs, but with opposite polarity: the positive side in IMM is the outer, rather than the inner aqueous side. $\Delta\mu_H^+$ couples respiration to the oxidative phosphorylation (OXPHOS) performed by the ATP synthase.

To build-up, maintain and utilize the delocalized $\Delta\mu_H^+$ for ATP synthesis, according to chemiosmotic theory (Mitchell 1966), a closed membrane vesicle with an inert, rigid and insulating membrane (Morelli et al. 2019) is required. This poses strong restrictions on the

ultrastructure and molecular organization of TMs and IMMs. Given the multiply folded, highly organized inner membrane systems of chloroplasts and mitochondria (see below), and their peculiar lipid compositions, with their major non-bilayer lipids, satisfaction of these conditions appears less straightforward than originally thought.

1.1.4. Ultrastructure

In vascular plants, TMs are differentiated into stacked, granum and unstacked, stroma regions. The grana are enriched in PSII and LHCII (light-harvesting complex II), complexes which possess small stroma-side protrusions and readily form extended ordered, often semi-crystalline macrodomains. In contrast, PSI and the ATP synthase, proteins with large protrusions to the outer aqueous side, are accommodated in the stroma TMs. By this lateral segregation, i.e. 'sorting' of the protein complexes according to the size of their stroma-side protrusions, stabilized by stacking, the packing density of TMs is substantially increased compared to random distribution of proteins. Members of the protein family, CURVATURE THYLAKOID 1 (CURT1) – via inducing and maintaining the extreme curvature at grana margins – also play pivotal role in shaping this highly organized TM ultrastructure.

The cylindrical grana stacks are (quasi-)helically wound around by stroma TMs (Fig. 2a), making membrane and lumenal connections between all layers of the grana, including the end membranes, which also contain PSI and the ATP synthase. Hence, with this organization, the granum and stroma TMs form a continuous membrane and enclose one interior (lumenal) aqueous phase, which is insulated from the stroma-side aqueous phase. Further, stroma TMs belonging to adjacent grana are also fused together (Fig. 2b).

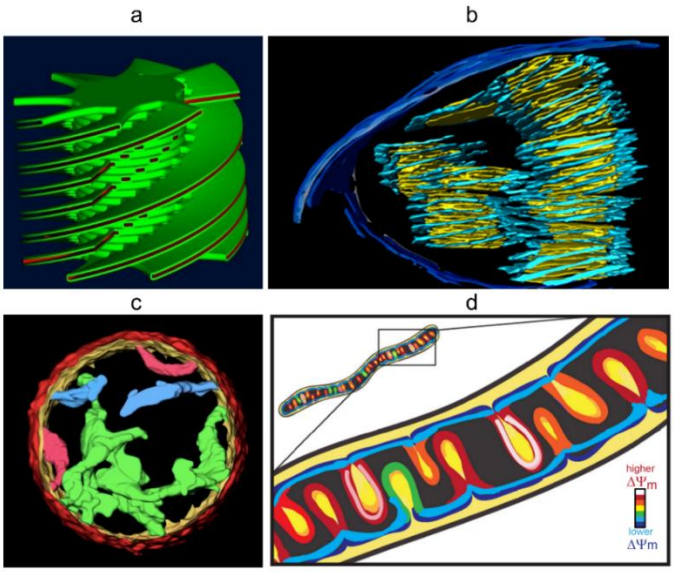

Fig. 2. Ultrastructural models of the granum-stroma thylakoid membrane assemblies (a, b) and the mitochondrial membranes (c, d).

IMM also displays a multiple-folded membrane system – compartmentalized into two distinct regions, the inner boundary membrane (IBM) and the cristae membrane (CM) (Fig. 2c). This heterogeneity has been correlated with a heterogenous distribution of the membrane proteins: components of the ETC, which are confined to the lateral surfaces of the CMs rather than equally distributed along the IMM, and dimers of the ATP synthase are found in rows along the edges of cristae. It has recently been shown that the mitochondrial membrane potential was higher in the CM than in the IBM and "cristae within the same mitochondrion behave as independent bioenergetic units" (Wolf et al. 2019) (Fig. 2d).

IMMs have high tendency for fusion and fission displaying high ultrastructural flexibility. The sizes and shapes of CMs are highly variable, they readily assume disk-like lamellar, tubular or bag-like structures. However, topology affects not only the OXPHOS efficiency but may create diffusional bottlenecks, limiting reaction rates inside mitochondria. In general, IMM surface area and topology respond to energy demand and different stresses (Mannella 2020).

1.1.5. Lipid composition

In TMs, the major lipids are galactolipids: monogalactosyldiacylglycerol (MGDG) and digalactosyldiacylglycerol (DGDG) account for about 50% and 30% of the total lipid content, respectively; they also contain sulfoquinovosyldiacylglycerol (SQDG) (~5–12%) and a phospholipid, the phosphatidylglycerol (PG) (~5–12%). As part of the adaptive response of TMs to different stress conditions, the lipid composition depends significantly on environmental factors.

IMMs contain only phospholipids (and no galactolipids). The three major phospholipids, in mammalian mitochondria, are phosphatidylcholine (PC, 40%), phosphatidylethanolamine (PE, 34%) and cardiolipin (CL, a diphosphatidylglycerol, 18%); as minor lipids, they also contain phosphatidylinositol (PI, 5%) and phosphatidylserine (PS, 3%). Plant cell mitochondria possess very similar lipid composition, with dominance of PC, PE and CL.

Although the (protein and) lipid compositions of the TMs and IMMs are markedly different, there are two common features shared by these membranes. First, their lipid-to-protein molar ratios are typically between 0.25-0.30. The other common, striking feature is that their major lipid species are non-bilayer lipids – MGDG, and PE and CL, respectively. These lipid species – in contrast to the cylindrically shaped bilayer lipids (DGDG, PG and SQDG in TMs and PC, PI and PS in IMMs) – due to their conical shapes, prefer not to form lamellar phases in the presence of water (Fig. 3a). Instead, they assemble into non-bilayer phases, such as cubic, isotropic or inverted hexagonal (H_{II}) phases These lipid phases exhibit characteristic ^{31}P-NMR spectra (Fig. 3b).

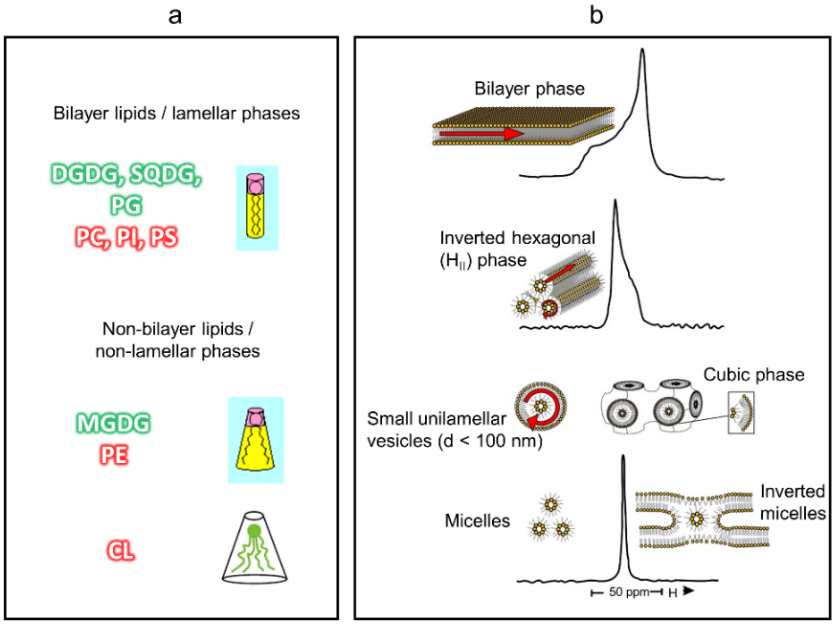

Fig. 3. Lipid species of TMs (green) and IMMs (red), which spontaneously assemble into bilayer or non-bilayer structures, according to their cylindrical or conical shapes, respectively (a) and ^{31}P-NMR signatures of the different lipid phases (b).

Information on the lipid polymorphism of membrane systems can be obtained by ^{31}P-NMR spectroscopy, which is a sensitive non-invasive technique to fingerprint the phase behavior of the bulk phospholipids *in vivo* and *in vitro*. Because of their restricted mobility compared to bulk lipids, this technique is largely insensitive to annular (or shell) lipids, constituting the first lipid layer around the membrane-intrinsic proteins, and even less to structure (or non-annular) lipids that are tightly bound to the proteins, and are typically found in cavities and grooves of protein hydrophobic regions. In TMs about 60% of the lipids are found in the fluid-like, bulk phase (Páli et al. 2003). According to a recent analysis, about 30% of total PG molecules in TMs are estimated to be found in photosynthetic protein complexes but >90% of total thylakoid lipids are located in the bulk phase (Yoshihara and Kobayashi 2022) or in the annular (shell) layer of the proteins.

1.1.6. Membrane models

The requirement that TMs and IMMs insulate the inner aqueous phases from the outer aqueous phases can be warranted by organizing the bulk lipid molecules into bilayer structures – as in the 'standard' fluid-mosaic model. The lipid bilayer possesses low permeability to water and most water-soluble molecules and to ions, and protons, in particular. However, within the frameworks of the 'standard' model, it is not straightforward to organize TM and IMM lipids into bilayers. This is because the 'standard' model does not take into account the occurrence of non-bilayer lipids in the membrane – a controversy that has been known for decades. It has been recognized that the phase behavior of isolated TM (and IMM) lipids cannot be extrapolated to biological membranes that are packed with proteins, which evidently stabilize the bilayer configuration.

Two models, the Lateral Pressure Model (LPM) (de Kruijff 1997), and the Flexible Surface Model (FSM) (Brown 2012), "challenge[d] the 'standard' model (the fluid mosaic model) found in biochemistry texts". LPM and FSM postulate that the presence of conically shaped non-bilayer lipids in the bilayer affect the structure and the functional activity of membrane-intrinsic proteins. According to LPM, non-bilayer lipids increase the lateral pressure in the hydrophobic region of the bilayer membranes and decrease it in the region of lipid headgroups. This pressure profile is proposed to "keep the [proteins] in a functional state, whereas in the absence of such force the proteins become less efficient or nonfunctional" (de Kruijff 1997). FSM predicts that "the non-lamellar-forming tendency of the membrane lipids modulates the protein energetics" due to variations in the curvature elastic energy. According to these models, non-bilayer lipids enhance the structural plasticity of membranes and lend dynamics to membrane-embedded proteins. At the same time, in these models the occurrence of non-bilayer lipid phases in the bilayer membranes is restricted only locally and transiently; i.e., neither LPM nor FSM consider persisting non-bilayer lipid phases inside the bilayer membrane or associated with it.

An alternative model, the Dynamic Exchange Model (DEM) (Garab et al. 2000, 2016, 2017) postulated that – in membranes composed of lipid molecules of high non-bilayer propensity – bilayer and non-bilayer lipid phases coexist and are in dynamic equilibrium with each other. DEM was based on two sets of experimentally and theoretically well founded premises: (i) the ability of membrane-intrinsic proteins to force non-bilayer lipids into the bilayer, and (ii) that when large protein-free membrane patches are exposed to water, the lipid molecules readily form transient structures, which are then segregated out from the membranes. As emphasized in (Garab et al. 2022 – listed), there are two additional features of DEM when applied for TMs and IMMs: (iii) they form closed membrane vesicles with their aqueous phases fully packed with proteins, some of which, especially those belonging to the class of lipocalins (or to lipocalin-like proteins), are capable of binding lipid molecules. and (iv) these vesicles are arranged into highly organized, extended networks.

1.2. Results

This chapter summarizes the main results and conclusions, which – with the exception of the effects of lipases and proteases (Dlouhý et al. 2022 – listed) – have been reviewed in (Garab et al. 2022 – listed), and in parts, focusing on the limitations of the fluid-mosaic membrane model (Wilhelm et al. 2020 – listed) and on the role of CL and non-bilayer lipid phases in IMMs as compared to TMs (Gasanoff et al. 2021). In this chapter, I will use primarily the scheme of presentation set in Ondřej Dlouhý's PhD thesis, which was defended on Februrary 22, 2023 at the University of Ostrava, Ostrava Czech Republic. When relevant, data on IMMs or its lipid model systems will also be mentioned.

I note here that, as stressed above, the lipid phase behavior of IMMs and TMs share many common features. Nonetheless, in the present Final Report, I confine the treatise on TMs and subchloroplast particles, mainly because our systematic experiments were limited to these materials. For results related to the polymorphic phase behavior of IMMs, see annual reports and a brief summary at the end of Chapter 1.2.

1.2.1. Lipid polymorphism of TMs

In our earlier works, we have established, using mainly ^{31}P-NMR spectroscopy (Krumova et al., 2008a, Garab et al., 2017) that TMs contain (at least) three well discernible individual spectral components – (i) lamellar (L) or bilayer phase peaking at around δP -12 ppm, (ii) inverted hexagonal (H_{II}) phase peaking at around δP 20 ppm and (iii) isotropic (I) phases peaking at around δP 3.9 and 4.6 ppm.

In recent years, we clarified that TMs obtained from plants belonging to different divisions and order possess similar features – indicating that lipid polimorphism of plant TMs is a ubiquitous feature.

We performed ^{31}P-NMR spectroscopy on a large number of TM batches (more than 100 preparations between 2018 and 2022), from spinach leaves; experiments performed in different seasons on three different 600 MHz spectrometers. The spectral distributions were very similar to those reported earlier (Garab et al., 2017). An average spectrum obtained from 14 different batches of freshly isolated spinach TMs is shown in Fig. **4**4. To discern each individual spectral components, we mathematically deconvoluted the spectra, which confirmed the above assignements: (i) L phase with an asymmetric shape, peaking at around δP -12 ppm with a downfield tail, (ii) an H_{II} phase, also with an asymmetric shape, peaking at around δP 20 ppm with an upfield tail, and (iii) I peaks with Lorentzian shapes peaking at around δP 2.7 (I_1) and 4.3 (I_2) ppm; some of our TM samples contained an intermediate isotropic (I_i) peak at around δP 3.5 ppm.

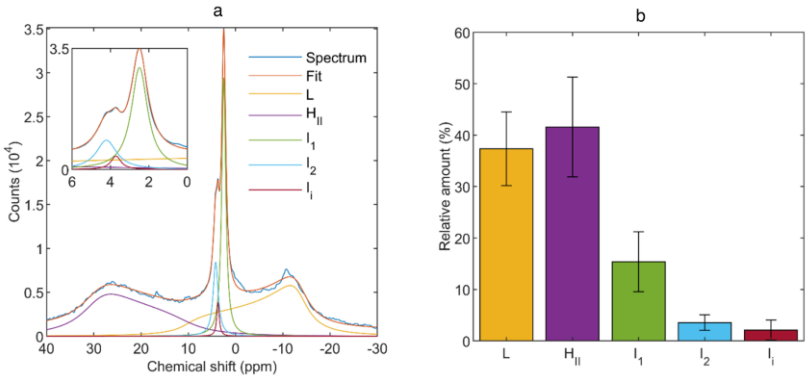

Fig. 4. ^{31}P-NMR spectrum (a) obtained after averaging spectra from independent batches of freshly isolated fully functional spinach thylakoid membranes (n=14) and relative amplitudes of the component spectra (b).

Quantitative analysis of the individual spectra, using the integrated areas of the component spectra, revealed that the amount of lipid molecules, associated with the H_{II} phase (42 ± 10 %) was as large as with the L phase (37 ± 7 %), and the rest of the bulk lipid molecules were found in I_1, I_2 and I_i phases, represented by about 15, 3 and 2 %, respectively (Fig. **4**b).

To rule out input bias of the mathematical deconvolution, we performed saturation transfer experiments. These experiments, as demonstrated in Fig. **5**5, confirm the validity of the spectral parameters obtained from the mathematical deconvolution.

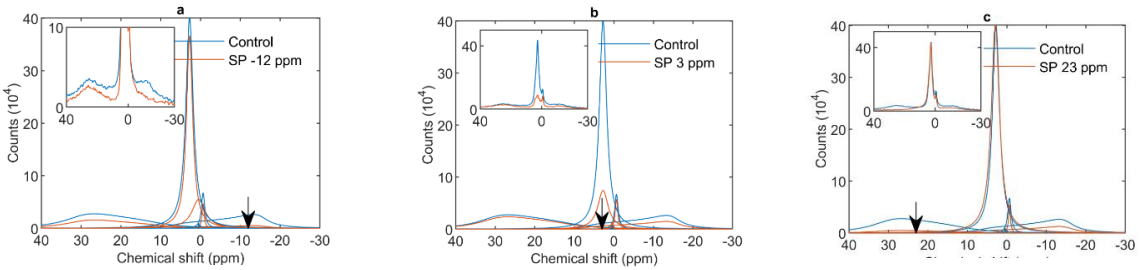

Fig. 5. Mathematically deconvoluted ^{31}P-NMR spectral components of isolated pea TMs: blue, before applying the saturating pulse (SP) and orange, with SP. The pulses were applied at frequencies shown by the arrows.

Earlier, it has been shown that the lipid polymorphism of isolated TMs is sensitive to changes in the osmotic and ionic strengths of the reaction medium; higher strengths increased the stability of the lipid phases (Garab et al., 2017). By comparing the stability of different lipid phases and the permeability of TMs in sorbitol- and NaCl-based reaction media, we confirmed higher stability of the bilayer phase in NaCl-based reaction medium; however, these samples displayed lower S/N ratio and also higher membrane permeability, evidently due to a higher basal ion flux across the membranes. Further, it became clear that the progressive weakening of L phase were correlated with increased membrane permeability. In general, these data, in accordance with the expectations, showed a close correlation between the membrane permeability, reflected by ΔA515 (electrochromic absorbance shift) decay kinetics, and the destabilization of the lamellar phase of isolated TMs, measured by 31P-NMR spectroscopy.

1.2.2. Subchloroplast particles

We clarified that the contribution of plastoglobuli to the lipid polymorphism of TMs is negligible. Hence, we ruled out the DLE model, suggesting dynamic lipid exchange between TMs and plastoglobuli (Kirchhoff 2019). We observed only a very weak sharp I signal of isolated plastoglobuli, which most probably originated from small phosphorus-containing molecules with rapid isotropic mobility, rather than from lipid-phase structures. These data allow us to conclude that the contribution of plastoglobuli to the lipid polymorphism of isolated TMs is negligible. This conclusion is consistent with data showing that the plastoglobuli contain only trace levels of TM lipids (van Wijk & Kessler, 2017). We cannot rule out that the trafficking of lipids between TMs and plastoglobuli participate in maintaining a constant lipid-to-protein ratio in TMs, as proposed in DLE (Kirchhoff, 2019). Such a mechanism might probably play a role in a long-term regulation of lipid content of TMs.

Membrane-embedded proteins and protein complexes may require different lipid phases for their proper function, as would be suggested by LPM and FSM. To test this hypothesis, we examined the lipid polymorphism of isolated granum and stroma sub-chloroplast particles, which are known to have the same lipid composition but to possess strikingly different protein compositions. Our ^{31}P-NMR spectra of isolated granum and stroma sub-chloroplast particles displayed virtually the same spectral components and very similar relative amplitudes of the

individual lipid phases as in whole TMs; these conclusions were confirmed by saturation transfer experiments and mathematical deconvolution. It is to be pointed out here that – despite a clear H_{II} signature in ^{31}P-NMR spectra of both granum and stroma TMs – there was no H_{II} signature seen using small-angle X-ray scattering (SAXS), indicating the lack of a long-range order of the H_{II} phase.

An interesting observation was that following the relatively harsh isolation procedures, both the granum and the stroma TM particles are able to re-seal, as seen by the induction and relaxation of ΔA515. These data indicate that the cleaved membranes are capable to fuse, and form closed vesicles with significantly high impermeability. To characterize the ultrastructure of isolated granum and stroma TMs, we used different electron microscopy techniques (scanning electron microscopy, SEM; freeze fracture electron microscopy, FF-EM; and cryo-electron tomography, CET). The acquired SEM images of granum and stroma TMs revealed the presence of small vesicles, connected via membrane fusions. Moreover, images obtained using FF EM and CET also provided evidence of interconnected membrane structures. The observed membrane fusions were suspected to give rise to one of the I phases.

1.2.3. Sensitivity of TM lipid phases to lipases

To further resolve the origin of individual lipid phases of TMs, and to test their susceptibility and accessibility to digestion, we applied Phospholipase A1 (PLA1), which is a phospholipid-selective lipase cleaving off the fatty acid at the sn-1 position from the glycerol backbone. Relatively low activity of the added enzyme (2 U mL^{-1}) rapidly (in 15 min) weakened all lipid phases. After 30-60 min, the L and H_{II} phases were completely digested, and the spectra were dominated by the newly emerged I bands peaking at around δP 1.5 and 3.3 ppm evidently originating from breakdown products.

Parallel with the gradual loss of the L phase, we observed a dramatic increase in membrane permeability. Short-term (≤ 60 min) treatment of TMs with 2 U mL^{-1} PLA1 did not induce any significant change in the structure and function of TMs – an observation that is in harmony with the compact organization of the multisubunit PSII and PSI supercomplexes that are largely retained even after detergent solubilization. Together with the highly similar lipid polymorphism of isolated granum and stroma TMs, these data allow us to rule out the dominant role of non-lamellar lipids of TMs in determining the functional activity and/or the modulation of protein energetics, as proposed in LPM and FSM, respectively. (Effects of longer PLA1 treatments, which are in accordance with earlier literature data, can be ascribed to the digestion of the non-annular PG molecules in key protein complexes.)

In contrast to PLA1, wheat-germ lipase (WGL) is substrate non-selective lipase. Interestingly, WGL, at 5 U mL^{-1}, selectively suppressed the I phases and, at the same time, formed a broad signal of immobilized lipids between δ_P 30 and -10 ppm. At higher activities (20 U mL^{-1}), WGL further suppressed the I phases and also diminished the L and H_{II} phases. At 5 U mL^{-1} WGL did not affect any of the monitored structural and functional parameters of TMs – in particular, it did not increase the membrane permeability, the distribution of excitation energy, the macro-organization of pigmen-protein complexes (PPCs), the activity of PSII and the PPC patterns of TMs. As in isolated spinach TMs, WGL of moderate activity added to isolated granum and stroma TMs selectively suppressed the I peak, and a new broad band, evidently originating from a largely immobile structure containing the digestion products, emerged. As in TMs, no changes in the monitored functional parameters of isolated granum and stroma TMs were seen.

Overall, these data strongly suggest that the WGL-susceptible I phase(s) is (are) to be found outside the protein-rich area containing the photosynthetic PPCs. This, together with EM images suggested that the I phase might originate from membrane fusions and junctions and/or bifurcations; a conclusion that is in line with the earlier tentative assignments of the I phase (Garab et al. 2017).

1.2.4. Sensitivity of TM lipid phases to proteinases

To examine the putative effects of interactions among membrane proteins on the lipid polymorphism of TMs, we treated the isolated TMs with Trypsin, selectively digests peptide bonds of stroma side TMs with limited or no access to the luminal membrane surface and thus, they are widely used to study protein topology in TMs. Unexpectedly, the H_{II} phase displayed a significant sensitivity to Trypsin, with just a minor or no effect on the other lipid phases. Parallel with this effect, a new broad phase centered around δP 15 ppm, extending between δP 40 and 20 ppm, emerged. Based on the shape and bandwidth of the newly emerged signal, we assigned it to large and mostly amorphic particles, with low molecular mobility and short transverse relaxation times. The specific susceptibility of H_{II} phase to Trypsin was confirmed by saturation transfer experiments and mathematical deconvolution. It is also important to point out that Proteinase K exerted very similar effect (Figure 6).

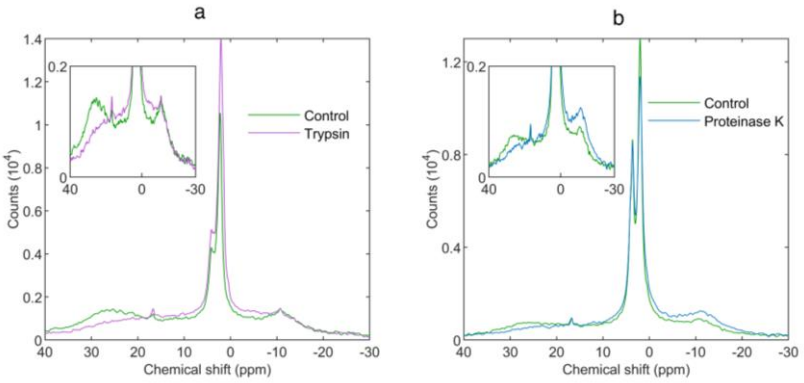

Fig. 6. ^{31}P-NMR spectra of spinach TMs untreated (Control, green) and treated with (a) 10 mg mL^{-1} Trypsin for 2 hours at 5 °C (purple); and (b) with 16 U ml^{-1} Proteinase K (blue) for 30 min at 22 °C. Insets highlight the H_{II} and L regions.

Data obtained from proteinase-treated TMs suggest that the H_{II} phase may originate from lipids surrounding and/or encapsulating stromal-side proteins and/or polypeptides which are loosely attached to TMs or protrude from a membrane-intrinsic protein. The identity of these proteins or polypeptides remains to be determined. It is interesting to note that earlier data have demonstrated that the water-soluble respiratory electron transport chain protein Cyt c is capable to induce H_{II} phase in association with CL, one of the major non-lamellar lipid of IMM (de Kruijff & Cullis 1980; Vladimirov et al. 2018). It is to be noted here that we have pointed out that cardiotoxin II might participate in intermembrane junction and have shown that the water-soluble small peptide melittin in a lipid model system affects the packing of IMM lipids. Short-chain alcohols have also been shown to perturb the organization of the bulk lpid molecules, especially in the presence of small polypetides.

1.2.5. Functional roles of non-bilayer lipid phases of TMs

Temperature is one of the most important environmental factors which can modulate the lipid composition of photosynthetic organisms and, vice versa, the lipid composition of TMs affects the temperature stress tolerance of the organism. Strong temperature dependence of the polymorphic phase behavior of TMs has earlier been demonstrated (Krumova et al. 2008a). We tested the reversibility of the temperature-induced changes via measuring the temperature-dependent behavior of TMs during cyclically switching the temperature between 5 and 15 °C.

Fig. 7a shows that temperature elevated from 5 to 15 °C caused an upfield shift of the I phases; the reversibility of these changes can be seen in Figure 7b. These temperature-induced reversible changes of the peak position, amplitude, and bandwidth are plotted in **Fig. 7**c. Upon elevating the temperature from 5 to 15 °C, the I peaks, besides shifting upfield, noticeably

broadened – which can be explained by the increase in the dynamics of the lipid transition between different phases at higher temperature; these changes were to a large extent reversible upon decreasing the temperature back to 5 °C.

Dependence of the light-induced generation and relaxation of ΔpH and ΔΨ during the cyclic switching between 5 and 15 °C showed that the membrane permeability increased, while the amplitudes were similar at 5 and 15 °C. In general, the acceleration of the decay of the pmf at higher temperature can most probably be accounted for higher mobility of the lipid molecules in the bilayer, which thus increases the permeability of membranes.

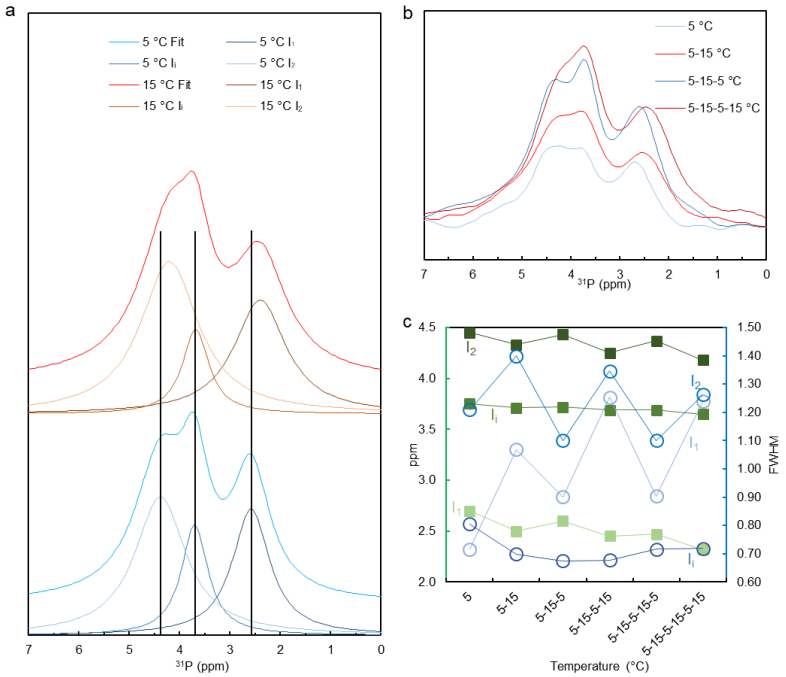

Fig. 7. ^{31}P-NMR spectra and spectral parameters (I region) of temperature-dependent variations of lipid phases of isolated thylakoid membranes.

During the operation of the linear ETC, the lumen can acidify by 2-3 pH units. Low pH-induced changes of the polymorphic phase behavior of TMs have earlier been demonstrated (Garab et al. 2017). As it was found earlier, the decrease of pH from 7.5 to 5.5 did not affect noticeably the L and H_{II} phases but caused an upfield shift of the I phases. It is an important finding that these changes were largely reversible (Figure 8).

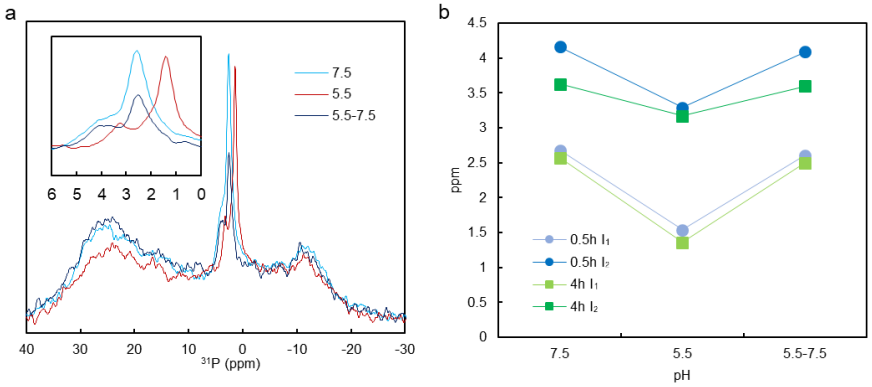

Fig. 8. (a) ^{31}P-NMR spectra of spinach TMs at pH 7.5, 5.5, and 7.5 after a 5 min incubation time at pH 5.5 (5.5–7.5); and (b) peak positions of the two isotropic peaks.

Data collected on temperature- and pH-induced variations in lipid polymorphism, and selected functional parameters of isolated TMs, were correlated with VDE activity of the membranes (VDE, violaxanthin de-epoxidase, which is a low-pH activated lumenal photoprotective enzyme). Our data revealed enhanced de-epoxidation rates at 15 °C and at low pH – despite the relaxation of the energized state (pmf) was accelerated under these conditions. These data led us to propose strong dependence of VDE on the enhancement of one of the I phases, and less on ΔpH. These data on TMs are in harmony with the findings on a lipid model system, which indicated the role of a non-bilayer (H_{II}) phase in the activity of VDE (Latowski et al. 2004).

1.3. Summary

In this OTKA project, we addressed basic questions about the structural and functional roles of the non-lamellar lipid phases in plant TMs – with the major aims to confirm and establish the fundamental characteristics of their lipid polymorphism, to identify structural entities responsible for the different lipid phases and to correlate the structural plasticity of lipid phases with physiologically important regulatory mechanisms of photosynthesis.

We performed ^{31}P-NMR spectroscopy, measured key parameters of the photosynthetic functions, and used a range of electron-microscopy, optical spectroscopy and biochemical analysis techniques to characterize basic features of our membrane preparations, which included freshly isolated TMs and granum and stroma sub-chloroplast particles. We also monitored the effects of different treatments, such as induced by variations in the temperature of samples, the pH of the media, and by lipases and proteinases.

By determining the ^{31}P-NMR spectral signatures of a large number of freshly isolated spinach TMs and analyzing them using mathematical deconvolution and saturation transfer protocols, we succeeded to confirm the co-existence of a lamellar and (at least) three non-lamellar lipid phases in spinach TMs; and to show very similar polymorphic profiles in higher plants belonging to different divisions and orders. We have shown that the granum / stroma lateral heterogeneity of TMs, and their strikingly different protein compositions, cannot be correlated with the polymorphism of TMs.

Regarding the origin of different lipid phases, our data have revealed that the observed non-lamellar phases are to be found in domains outside the protein-rich areas that contain the lipid-bilayer embedded super-complexes performing the light reaction of energy conversion. The role of plastoglobuli, as a possible source of non-lamellar lipid phases was ruled out.

Our data strongly suggest, that in accordance with earlier, tentative assignments, the isotropic non-lamellar phases are involved in membrane fusions and junctions; and originate from association of lipid molecules with lipocalins or lipocalin-like proteins in the aqueous phase of the TM vesicles, including the water-soluble enzyme VDE. Further, we have shown that the inverted hexagonal (H_{II}) phase (or at least large part of it) is generated by lipid molecules surrounding and/or encapsulating stromal-side proteins or polypeptides. These data show that non-lamellar lipid phases play important roles in the self-assembly of the TM system, which forms a highly organized multilamellar membrane network; and that lipid molecules are associated with proteins and/or polypeptides both in the inner and the outer aqueous phases of these energy-converting membrane vesicles.

We revealed reversible temperature- and pH induced enhancements of the isotropic phase(s). In reasonable accordance with model-membrane experiments, the enhanced non-lamellar isotropic phase in TMs could be correlated with the modulation of the activity of VDE in the xanthophyll cycle and in the photoprotective non-photochemical quenching mechanism. These lipid-phase variations appeared to overwhelm the increased permeability of TMs at low pH and at elevated temperatures – pointing to the physiological importance of the structural dynamics of the bulk lipid phases of TMs.

We also tested the presently available membrane models which had been proposed to complement the standard fluid-mosaic model by taking into account the presence of non-lamellar lipids in biological membranes. Our data are at variance with the proposed membrane models confining the role of non-lamellar lipids in the membrane bilayer – either to maintain the activity of the membrane-intrinsic proteins via the lateral pressure exerted by these lipids (LPM), or to regulate the energetics of membrane proteins via forming flexible surfaces (FSM); the model (DLE), proposing dynamic lipid exchanges between plastoglobuli and TMs were also found to be inconsistent with experimental data. On the other hand, our conclusions are in harmony with DEM of TMs, a model which proposes dynamic exchange between different lipid phases, safe-guarding the lipid-to-protein ratio of TMs and contributing to the overall structural plasticity of membranes.

Finally, I would like to emphasize that while „further research is needed to identify and characterize the structural entities associated with the observed non-bilayer phases in IMMs and TMs and that albeit fundamental questions remain to be elucidated, non-lamellar lipid phases should be considered on a par with the bilayer phase, with which they co-exist in functional TMs and IMMs" (Garab et al. 2022). (For details on IMMs, see annual reports.)

Related publications (in chronological order): Ughy et al. 2019, Wilhelm et al. 2020, Dlouhý et al. 2020, Gasanoff et al. 2021 (a,b), Dlouhý et al. 2021 (a,b), Dlouhý et al. 2022, Wang et al. 2022, Garab et al. 2022, Dlouhý 2023 (PhD thesis).

2. Additional results

In this section, I will briefly outline results obtained with the support of the present OTKA proposal. Some of these works are tightly, others are only loosely connected with the main topic of the Project. The obtained data may aid us in our future work to better understand the self-assembly, molecular organization and structural/functional plasticity of the photosynthetic machineries at different levels of complexity – i.e., in recognizing broader contexts of the structural and functional roles of non-bilayer lipids and non-lamellar lipid phases in TMs; the methodological papers are also of significant value.

2.1. Macro-organization of TMs

As pointed out in Section 1, the self-assembly and structural dynamics of TMs depend on the presence of non-bilayer lipids and non-lamellar lipid phases. It is equally important to understand other factors that determine the ultrastructure of TMs and the macro-organization of PPCs (Note that characteristic parameters have been measured in most cases also in Section 1).

We provided an overall review on the stability and plasticity of PSII in different molecular environments and correlate our findings with the evolution of multilevel regulatory processes of the photosynthetic machinery of thylakoid membranes.

We have pointed out that TMs should not be considered to be a scaffold system containing the PPCs and other constituents of the light-energy converting machinery but their active participation in regulatory processes should always be considered. This became evident e.g., via employing the non-invasive technique of SANS on the climbing rainforest evergreen vine *Monstera deliciosa* leaf segments. We have revealed light-induced remodelling of the thylakoid membrane system under NPQ-inducing illumination conditions. Our measurements revealed a substantial diminishment of the long-range, periodic order of granum thylakoid membranes; these changes were almost fully and rapidly reversible in the dark.

We have revealed the role of protein-water interface in the stacking interactions of granum thylakoid membranes via investigating the effects of Hofmeister salts on the organization of PPCs and on the ultrastructure of thylakoid membranes. We found that kosmotropic and

Hofmeister-neutral salts, up to 2 M concentrations, hardly affected the macro-organization of the protein complexes and the membrane ultrastructure. In contrast, chaotropic salts destroyed the mesoscopic structures, the multilamellar organization of the thylakoid membranes and the chiral macrodomains of the protein complexes but without noticeably affecting the short-range, pigment-pigment excitonic interactions.

Via monitoring the macro-organization of thylakoid membranes, using TEM, SANS and CD spectroscopy, and determining the pigment- and protein-composition of membranes, and measuring the activity of the photochemical apparati, using absorption and Chl-a fluorescence transients. Our data have shown that beside strong similarities of the toxic effects of Cr and Cd, the response of the photosynthetic machinery of C. variabilis to these two trace metal ions substantially differ from each other.

We also studied the effects of salt stress on the growth, morphology, photosynthetic performance in the mixotrophic, unicellular, flagellate Euglena gracilis. Our CD spectroscopy data revealed changes in the macro-organization of PPCs due to salt treatment, while SANS and TEM data revealed changes in TM stacking.

Related publications (in chronological order): Zsiros et al. 2020 a,b, Ünnep et al. 2020, Lambrev et al. 2021, Kanna et al. 2021.

2.2. Lipid-protein interactions

Proteo-liposomes were used to study the dependence of chlorophyll fluorescence quenching on the lipid-to-protein ratio in reconstituted LHCII membranes. The liposome also contained a lipid label fluorescence marker molecule and the lipid-to-protein (L/P) ratio was also measured. A strong correlation was found between the fluorescence quenching and the L/P ratio, presumably triggered by self-clustering in the membrane.

The accumulation of geranylgeranylated Chls a and b in the PPCs of Arabidopsis plants acclimated to green light brought about structural–functional consequences on the photosynthetic apparatus: it hampered the formation of PSII and PSI super- and megacomplexes; which is explained by the fact that phytol chains mediate contact with fatty acids, as main interaction between lipid molecules and Chl a in PSII core; hence replacing phytyl with an unsaturated geranylated chain could contribute to PSII core instability.

In a series of works, the rate-limiting steps (discovered in our laboratory) in the dark-to-light transition of PSII has been characterized in detail by a range a biophysical techniques, revealing that PSII RCs, in addition to the open and closed state, can assume a light-adapted charge-separated (closed) state that possess higher stability of charges. It has been shown that these transitions depend largely on the lipid content of the RC matrix.

Related publications (in chronological order): Akhtar et al. 2019 (Chem Phys), Sipka et al. 2019, Sipka et al. 2021, Karlický et al. 2021, Sipka et al. 2022, Magyar et al. 2022.

2.3. Methodology

Liposome-embedded LHCII was used to measure the anisotropic circular dichorism (ACD) in the UV-VIS region – showing that ACD reveals additional information about the excited states that is lost in the CD of randomly oriented solutions. ACD spectra have revealed drastically enhanced magnitudes of some bands and details compared to the isotropic CD spectra, resolving a greater number of bands and weak optical transitions – thus making ACD spectroscopy a valuable tool linking the three-dimensional structure and the photophysical properties of PPCs.

Advancement and use of differential polarization (DP) laser-scanning microscopy, combining modern microscopy imaging with polarization spectroscopy, has been reviewed. DP imaging provides unique and quantitative information on the anisotropic molecular organization of plant

cell constituents – and might also be used to monitor the polymorphic phase behavior of thylakoid membranes and /or of model membranes possessing different bulk lipid phases.

Recent advancements and future perspectives of the non-invasive technique SANS in photosynthesis research were overviewed. SANS provides statistically and spatially averaged structural information on the mesoscopic scale about TMs in vitro and in vivo and about regulatory mechanisms fine-tuning the photosynthetic functions and affecting the organization of TMs at different levels of the structural complexity under physiologically relevant conditions, without fixation or staining. It has been demonstrated and used that SANS reveals rapid reversible reorganizations on the timescale of several seconds and minutes.

Related publications (in chronological order): (Akhtar et al. 2019 JPC), Nagy and Garab 2021, Radosaljevič et al. 2021.

Cited References:

Brown, M.F. (2012) Curvature Forces in Membrane Lipid-Protein Interactions. Biochemistry 51: 9782-9795.

de Kruijff, B. (1997) Biomembranes - Lipids beyond the bilayer. Nature 386: 129-130.

de Kruijff, B. and P.R. Cullis (1980) Cytochrome c specifically induces non-bilayer structures in cardiolipin-containing model membranes, Biochimica et Biophysica Acta - Biomembranes 602: 477-490.

Garab, G, K. Lohner, P. Laggner, T. Farkas (2000) Self-regulation of the lipid content of membranes by non-bilayer lipids: a hypothesis, Trends Plant Sci 5: 489-494.

Garab, G, B. Ughy, R. Goss (2016) Role of MGDG and Non-bilayer Lipid Phases in the Structure and Dynamics of Chloroplast Thylakoid Membranes, Subcell Biochem 86: 127-157.

Garab, G, B. Ughy, P. de Waard, P. Akhtar, U. Javornik, C. Kotakis, P. Šket, V. Karlický, Z. Materová, V. Špunda, J. Plavec, H. van Amerongen, L. Vigh, H. Van As, P.H. Lambrev (2017), Lipid polymorphism in chloroplast thylakoid membranes - as revealed by P-31-NMR and timeresolved merocyanine fluorescence spectroscopy, Sci Rep 7.

Gasanov, S.E., A.A. Kim, L.S. Yaguzhinsky, R.K. Dagda (2018) Non-bilayer structures in mitochondrial membranes regulate ATP synthase activity. Biochim Biophys Acta 1860: 586-599.

Krumova, S.B., C. Dijkema, P. de Waard, H. Van As, G. Garab, H. van Amerongen (2008a) Phase behaviour of phosphatidylglycerol in spinach thylakoid membranes as revealed by P-31-NMR. Biochim Biophys Acta 1778: 997-1003.

Krumova, S.B., R.B.M. Koehorst, A. Bóta, T. Páli, A. van Hoek, G. Garab, H. van Amerongen (2008b) Temperature dependence of the lipid packing in thylakoid membranes studied by time- and spectrally resolved fluorescence of Merocyanine 540. Biochim Biophys Acta 1778: 2823-2833.

Latowski, D., H.-E. Akerlund, K. Strzalka (2004) Violaxanthin de-epoxidase, the xanthophyll cycle enzyme, requires lipid inverted hexagonal structures for its activity. Biochemistry 43: 4417-4420.

Mannella, C.A. (2020) Consequences of Folding the Mitochondrial Inner Membrane. Front Physiol 11: 536.

Mitchell, P. (1966) Chemiosmotic coupling in oxidative and photosynthetic phosphorylation. Biol Rev Camb Philos Soc 41: 445-502.

Morelli, A.M., S. Ravera, D. Calzia, I. Panfoli (2019) An update of the chemiosmotic theory as suggested by possible proton currents inside the coupling membrane. Open Biology 9: 180221.

Páli, T., G. Garab, L.I. Horváth, Z. Kóta (2003) Functional significance of the lipid-protein interface in photosynthetic membranes. Cell Mol Life Sci 60: 1591-606.

Singer, S.J. and G.L. Nicolson (1972) The Fluid Mosaic Model of the Structure of Cell Membranes. Science 175: 720-731.

Wolf, D.M., M. Segawa, A.K. Kondadi, R. Anand, S.T. Bailey, A.S. Reichert, A.M. van der Bliek, D.B. Shackelford, M. Liesa, O.S. Shirihai (2019) Individual cristae within the same mitochondrion display different membrane potentials and are functionally independent. EMBO J 38: e101056.

Yoshihara, A. and K. Kobayashi (2022) Lipids in photosynthetic protein complexes in the thylakoid membrane of plants, algae, and cyanobacteria. J Exp Bot 73: 2736-2750.